REVIEWS

Theory-guided design of catalytic materials using scaling relationships and reactivity descriptors

Zhi-Jian Zhao [1,2], Sihang Liu [1,2], Shenjun Zha[1,2,3,4], Dongfang Cheng [1,2], Felix Studt[3,4], Graeme Henkelman[5] and Jinlong Gong [1,2] *

Abstract | The active sites of heterogeneous catalysts can be difficult to identify and understand, and, hence, the introduction of active sites into catalysts to tailor their function is challenging. During the past two decades, scaling relationships have been established for important heterogeneous catalytic reactions. More specifically, a physical or chemical property of the reaction system, termed as a reactivity descriptor, scales with another property often in a linear manner, which can describe and/or predict the catalytic performance. In this Review, we describe scaling relationships and reactivity descriptors for heterogeneous catalysis, including electronic descriptors represented by d-band theory, structural descriptors, which can be directly applied to catalyst design, and, ultimately, universal descriptors. The prediction of trends in catalytic performance using reactivity descriptors can enable the rational design of catalysts and the efficient screening of high-throughput catalysts. Finally, we outline methods to break scaling relationships and, hence, to break the constraint that active sites pose on the catalytic performance.

[1]Key Laboratory for Green Chemical Technology of Ministry of Education, School of Chemical Engineering and Technology, Tianjin University, Tianjin, China.

[2]Collaborative Innovation Center of Chemical Science and Engineering, Tianjin, China.

[3]Institute of Catalysis Research and Technology, Karlsruhe Institute of Technology, Hermann-von-Helmholtz-Platz 1, Eggenstein-Leopoldshafen, Germany.

[4]Institute for Chemical Technology and Polymer Chemistry, Karlsruhe Institute of Technology, Karlsruhe, Germany.

[5]Department of Chemistry and the Oden Institute for Computational Engineering and Sciences, University of Texas at Austin, Austin, TX, USA.

*e-mail: jlgong@tju.edu.cn

Heterogeneous catalysis, in which the rate of a specific reaction is accelerated by a catalyst, plays an important role in the chemical industry[1–3]. Developing a suitable catalyst is the first step to industrialize a catalytic process. Traditional approaches for catalyst design rely on trial-and-error tests because of the complex structures of supported catalysts and the limited in situ characterization technologies.

Nowadays, computational modelling provides a more rational way to design catalysts. Using density functional theory (DFT) and other theoretical methods, reaction mechanisms at the molecular level can be determined. Concurrently, the discovery of scaling relationships between properties of catalytic materials and the stability of the reactive intermediates have furthered our knowledge of the catalytic process. More specifically, studies have investigated the electronic structure of the catalyst, the binding strength of intermediates on the surface and a range of geometric properties. These scaling relationships reveal the factors that influence the catalytic trends of different materials. Based on the scaling relationships, researchers can choose one or a few properties, termed reactivity descriptors, to correlate surface-reaction energies and activation barriers. In this way, a high-dimensional kinetic model based on the activation and reaction energies of all elementary reaction steps is reduced to a few dimensions described by a series of reactivity descriptors, which can predict trends in catalytic performance.

Using scaling relationships to construct reactivity descriptors has been intensively investigated (FIG. 1). The timeline includes the earliest electronic descriptor based on d-band theory for transition-metal catalysts, which links the binding strength of reaction intermediates and the d-band electronic structure of the metal[4–6]. The timeline details the development of electronic descriptor, structural descriptors, binary descriptors (in which both electronic and structural properties are considered) and elementary universal descriptors[7–10]. In this Review, we discuss reactivity descriptors in different catalytic systems, taking into consideration the limitations of scaling relationships and strategies to break these established scaling relationships. In addition, we aim to lay foundations for the future computational design of catalysts.

d-band theory

The d-band model aids our understanding of bond formation and chemical reactivity in catalysis[4–6,11,12]. In the 1990s, the relationship between the electronic properties of metals and their chemical reactivity began to be established. A landmark publication provided an explanation for the noble properties of gold by Hammer and Nørskov[4]. Since then, d-band theory has been widely

used to describe bond formation on transition-metal surfaces, which have different filling of the *d* band. Considering the interaction between the metal surface and adsorbates, the coupling to the broad-metal *s* band leads to a broadening and downward shift of the electronic states of the adsorbate (FIG. 2a). In general, the higher the *d* states are in energy relative to the Fermi level, the higher the antibonding states are in energy and the stronger the bond is between the adsorbate and the metal surface. This principle has been adopted to interpret catalytic properties based on the analysis of electronic structures of the corresponding active sites.

To improve the description of the energy level of the *d* band of a metal surface, the average energy of the band,

namely, the *d*-band centre, was introduced into *d*-band theory[13,14]. By calculating the *d*-band centre of a metal surface, the adsorbate–metal interaction can be qualified as follows: a metal site with a higher (lower) *d*-band centre exhibits stronger (weaker) affinity towards adsorbates because of the decreased (increased) filling of adsorbate–metal antibonding states. For example, if the subsurface of Pt(111) is replaced by another metal, the *d*-band centres of the surface Pt atoms are shifted[14]. Interestingly, the *d*-band centres of surface Pt scale well with the dissociative adsorption energy of H_2 and O_2. With a less negative *d*-band centre, the dissociative adsorption strength becomes stronger. These results are useful for catalyst design, for example, for proton-exchange membrane fuel
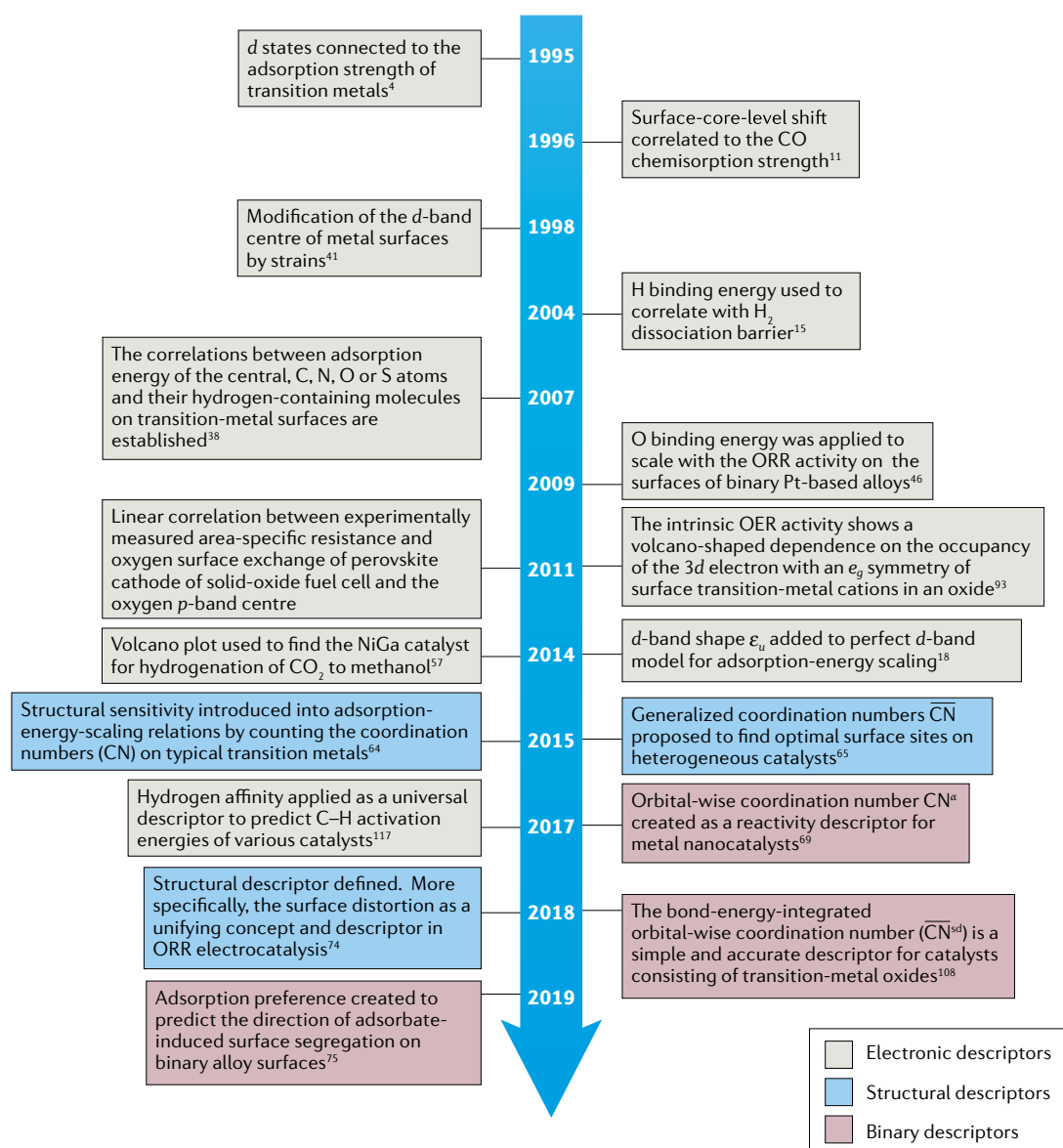
1995 — *d* states connected to the adsorption strength of transition metals[4]

1996 — Surface-core-level shift correlated to the CO chemisorption strength[11]

1998 — Modification of the *d*-band centre of metal surfaces by strains[41]

2004 — H binding energy used to correlate with H_2 dissociation barrier[15]

2007 — The correlations between adsorption energy of the central, C, N, O or S atoms and their hydrogen-containing molecules on transition-metal surfaces are established[38]

2009 — O binding energy was applied to scale with the ORR activity on the surfaces of binary Pt-based alloys[46]

2011 — Linear correlation between experimentally measured area-specific resistance and oxygen surface exchange of perovskite cathode of solid-oxide fuel cell and the oxygen *p*-band centre

The intrinsic OER activity shows a volcano-shaped dependence on the occupancy of the 3*d* electron with an e_g symmetry of surface transition-metal cations in an oxide[93]

2014 — Volcano plot used to find the NiGa catalyst for hydrogenation of CO_2 to methanol[57]

d-band shape ε_u added to perfect *d*-band model for adsorption-energy scaling[18]

2015 — Structural sensitivity introduced into adsorption-energy-scaling relations by counting the coordination numbers (CN) on typical transition metals[64]

Generalized coordination numbers $\overline{CN}$ proposed to find optimal surface sites on heterogeneous catalysts[65]

2017 — Hydrogen affinity applied as a universal descriptor to predict C–H activation energies of various catalysts[117]

Orbital-wise coordination number CN^α created as a reactivity descriptor for metal nanocatalysts[69]

2018 — Structural descriptor defined. More specifically, the surface distortion as a unifying concept and descriptor in ORR electrocatalysis[74]

The bond-energy-integrated orbital-wise coordination number ($\overline{\overline{CN}}^{sd}$) is a simple and accurate descriptor for catalysts consisting of transition-metal oxides[108]

2019 — Adsorption preference created to predict the direction of adsorbate-induced surface segregation on binary alloy surfaces[75]

Legend:
- ☐ Electronic descriptors
- ☐ Structural descriptors
- ☐ Binary descriptors

Fig. 1 | **A timeline of the development of reactivity descriptors and scaling relationships in heterogeneous catalysis.** Reactivity descriptors first appeared with the interpretation of the electronic states of catalytic systems. For example, the classic *d*-band theory directly links the electronic properties of metals to their reactivity in catalysis. Structural descriptors regulate reactivity by modifying the surface structures of catalysts. Binary descriptors simultaneously consider the electronic and structural properties of the catalytic systems and describe or predict the reaction trends more accurately. OER, oxygen evolution reaction; ORR, oxygen reduction reaction.
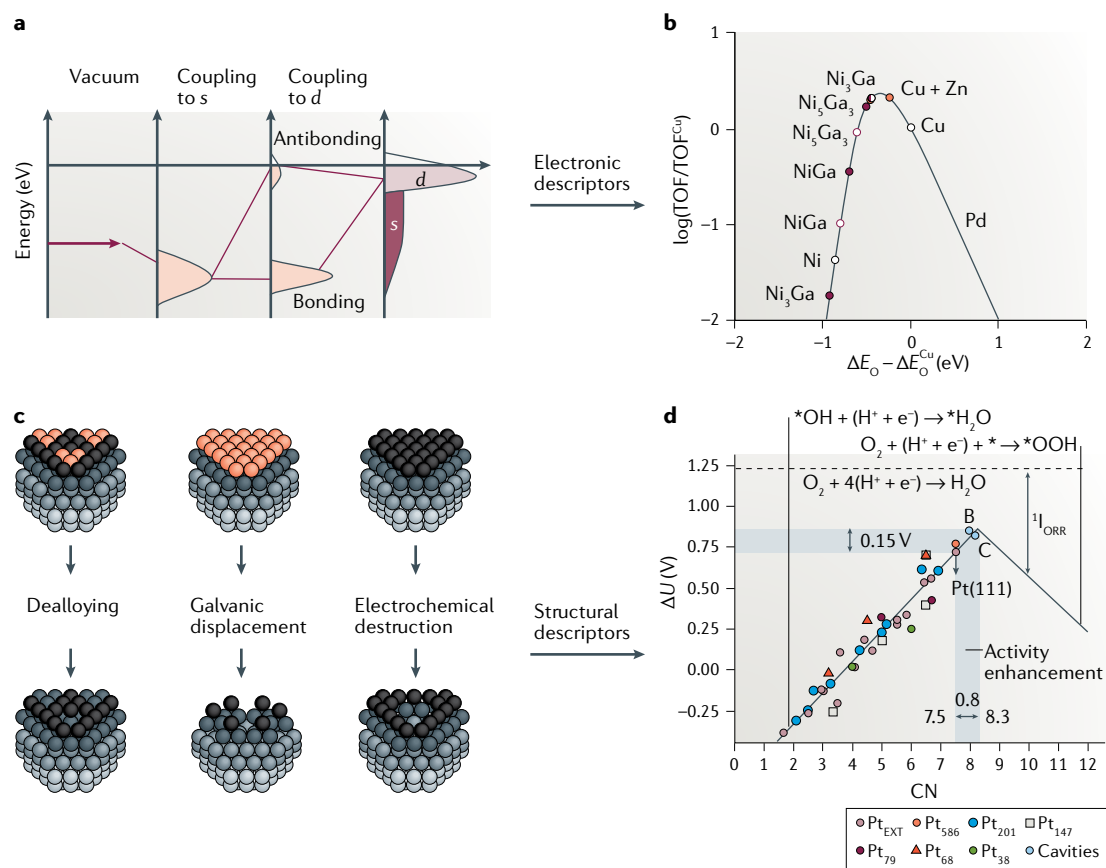
Fig. 2 | **Typical reactivity descriptors in metallic catalysts. a** | A schematic illustration of bond formation at a transition-metal surface. The lower the d states are in energy relative to the Fermi level, the more filled the antibonding states and the weaker the adsorption bond. **b** | A theoretical volcano curve for the activity of hydrogenation of CO_2 to methanol. The turnover frequency (TOF) is plotted as a function of the adsorption energy of *O (ΔE_O) on different surfaces, relative to Cu(211). **c** | Schematics of the approaches used to create defects at Pt(111) surfaces. Cu atoms are red and Pt atoms are grey or black, according to the depth with respect to the surface layer. **d** | Potentials (ΔU) for the two limiting steps on Pt extended surfaces and nanoparticles and two Pt surface cavities. CN, coordination number. Part **a** is adapted from REF.[9], Springer Nature Limited. Part **b** is adapted from REF.[57], Springer Nature Limited. Parts **c** and **d** adapted with permission from REF.[65], AAAS.

cell electrocatalysts[15,16], as well as the dehydrogenation of propane[17].

As well as the position of the d-band centre, other factors affect the applicability of the d-band model. For example, the width and the shape of the d band, which are governed by the local geometry and composition of materials, have important roles in determining the surface reactivity of transition-metal alloys[18,19]. There is a similar correlation between adsorbate-interaction energies and the substrate d-band centre for transition-state energies. Adsorption and transition-state energies are governed largely by the same intrinsic, electronic structure properties of a specific surface and, hence, it is expected that the correlations between reaction energies and activation energies, the so-called Brønsted–Evans–Polanyi (BEP) relation[20–30], are prevalent on metal surfaces. With known scaling relationships, the energy barriers can be predicted by calculating the adsorption energies of all the involved species. However, the existence of the BEP relationship limits the modulation of the overall reaction-energy profile, because the strong binding of transition states is correlated with the strong binding of reactants. How to break the limits of such scaling relationships is a bottleneck question.

Descriptors on metal surfaces

The interaction strength between reactant molecules and catalytic surfaces is described by the adsorption energy[22], which can be measured accurately by surface-science techniques. In addition, DFT with its derivative calculation methods and the assistance of machine learning provide remarkable computing power to calculate the adsorption energies of different systems[31–37]. However, the potential number of reactive species can be very large and an exhaustive calculation of all adsorption energies is daunting for most applications. To solve this problem, the interrelation of various adsorption energies has been carefully explored. For example, the adsorption strengths of CH_x, $x = 0, 1, 2, 3$, NH_x, $x = 0, 1, 2$, OH_x, $x = 0, 1$ and SH_x, $x = 0, 1$ were computed on multiple representative transition-metal surfaces[38]. The adsorption energies of these hydrogenated molecules correlate well with the adsorption energies of the central atoms (C, N, O or S). The nature of these scaling relationships is attributed to a synchronous variation of valence electrons of metal surfaces and adsorbates, and accounts for the similarity of the changing trends of adsorption strength between ZH_x (where $Z = C, N, O$ or S)[39].

From this point of view, the scaling relationships for different sets of adsorption energies are substantially influenced by electronic properties[6,16,40-42].

Focusing on a specific reaction, the adsorption energies of key intermediates affect both the activity and the selectivity. If reactants adsorb too strongly, this overbinding may poison the surface and slow the reaction; if reactants bind too weakly, the related transition states will be energetically high, thus limiting the overall activity. This golden rule, or the Sabatier principle, attributes outstanding catalytic performance to moderate adsorption energies of key reaction intermediates[43-45]. By modifying the adsorption energies of important reactive species, we can direct the reaction towards the desired products and avoid unwanted side reactions[7,46,47]. A volcano relationship between the calculated oxygen adsorption and the measured kinetic-current density of Pt-based bimetallic catalysts for the oxygen reduction reaction (ORR) was discovered[48]. Interestingly, the adsorption energy of oxygen scales roughly with the two key reaction intermediates, *OH and *OOH. Therefore, the adsorption energies of oxygen simultaneously control the stability of Pt–OOH and the Pt–OH or Pt–O bonds, resulting in the opposite trend of ΔG for the first two elementary steps. The above scaling relationship has been successfully confirmed by experimental study[49]. In addition, computational design in hydrogen evolution reaction (HER) catalysts uses the adsorption strength of H as an activity descriptor to guide the catalyst screening, which successfully identifies new electrocatalysts through theory-based and high-throughput processes[50-53]. More recently, a fully automated screening method that combines machine learning with DFT calculations has guided the discovery of electrocatalysts for CO_2 reduction and H_2 evolution, during which the adsorption strength of CO and H have been used as reactivity descriptors[54].

Reactivity descriptors derived from adsorption energies are easy to calculate and reflect the energy landscape of a reaction system. For the semi-hydrogenation of acetylene, there is a linear relationship between the adsorption strengths of C_2H_x (where $x = 2, 3, 4$ or 5) and the adsorption strength of methyl groups. To enhance the conversion of acetylene to ethylene and the selectivity towards ethylene, a good catalyst should have moderate adsorption strength for methyl groups. Based on this scaling relationship, a set of alloy catalysts for selective hydrogenation of acetylene, NiZn alloys, was discovered[55]. Another example of using the adsorption energy of key intermediates is to select promising catalysts for CO_2 conversion to methanol. The complicated mechanism of the CO_2 hydrogenation reaction makes it difficult to determine the interplay of all possible elementary steps[56]. To catalyse methanol production from CO_2 hydrogenation, bimetallic catalysts show outstanding activity and selectivity compared with their single-metal counterparts; for example, the discovery of a NiGa catalyst for the reduction of CO_2 to methanol at ambient pressure[57]. The turnover frequencies of various metal catalysts are plotted as a volcano-like function of the adsorption energy of oxygen, ΔE_O, on stepped 211 surfaces of the catalysts (FIG. 2b). The shape of this volcano-like relationship is based on the adsorption energies of formate species and other oxygen-binding species on the surfaces. As a result, the optimum catalyst has moderate oxygen adsorption strength. Compressing a complex reaction pathway into one or two simple adsorption descriptors not only grasps the nature of a specific reaction and reduces complex analysis but also provides a clear direction for computational catalyst design. The electronic descriptors on the metal catalysts have such a diverse spectrum, covering both d-band theory and the adsorption energies of key reaction species. Other electronic descriptors include charge polarization[58] and the average $2p$-state energy[59]. Because of this, more intuitive and controllable properties should be introduced as potential descriptors.

Inspired by the structure–sensitivity property of certain reaction systems, the idea of structural descriptors has been raised[22,60-63]. Structural descriptors connect the geometric structure of optimal active sites with catalytic performance, making it possible to design catalysts by constructing specific active sites. The coordination numbers (CNs) of the binding atoms in active sites scale with the adsorption energies on extended surfaces with various facets or defects. The CNs of specific active sites exhibit linear scaling relationships with the adsorption energies of oxygen and oxygenates on the ubiquitous transition metals in catalysis[64]. By counting the CNs of the atoms of the active sites, the binding strength towards reaction intermediates can be predicted, which is then transferred to adsorption–energy scaling relationships to predict catalytic reactivity. However, because of finite-size effects in nanoscale systems, CNs are sometimes inaccurate for small nanoparticles. To solve this problem, the concept of generalized CN ($\overline{CN}$) was introduced to design Pt-based catalysts in ORRs[65]. The $\overline{CN}$ extends the counting of nearest neighbours to weighting each first-nearest neighbour corresponding to its CN. By fabricating defective Pt(111) surfaces (FIG. 2c), ORR performance was improved, with an increased number of second-nearest neighbours of surface Pt atoms. The adsorption free energies of ORR intermediates on Pt nanoparticles of various sizes scale with the $\overline{CN}$. Remarkably, the rate-limiting potentials in the ORR have a volcano-shaped relationship with $\overline{CN}$, and Pt nanoparticles with cavities display a 0.15-V activity enhancement compared with a Pt(111) reference (FIG. 2d). This study paves the way for designing high-performance catalysts using structural descriptors, for example, the CNs of active sites. The incorporation of structural and electronic descriptors is particularly promising for predicting reactivity and building high-performance catalysts[66-68].

Based on the foundation of using CNs as a descriptor, the orbital-wise CN (CN^α, $\alpha = s$ or d) has been developed as a more accurate reactivity descriptor for metal nanocatalysts[69]. The CN^α quantifies the degree of coordinative saturation of metal atoms and their tendency to form bonds via the α orbital of a specific adsorption site. This upgraded descriptor based on CN^α can be applied to complex systems with varying lattice strains and metal ligands, because it considers both the geometric and the electronic structures of active sites.

The approach of calculating CNs of active sites has inspired advances in the prediction of activity and catalyst screening[66,70–73]. More specifically, surface distortion has been discovered to be a unifying reactivity descriptor in ORR electrocatalysis using PtNi/C catalysts[74]. By tuning the surface defects of bimetallic alloys, a highly active and sustainable ORR catalyst can be designed. Recently, the concept of adsorption preference of a binary alloy surface has been proposed, defined as the adsorption-strength difference of an adsorbate on different pristine metal surfaces[75]. This descriptor connects the adsorption strengths of surface species with the surface structure of the catalysts, which is regarded as another binary descriptor. Adsorption preference can be applied to determine the segregation direction, providing a more reliable surface model under reaction conditions than the single-crystal surface model. This adsorption preference descriptor is indirectly linked to reactivity, but can be used to rationalize the alloy surface with various adsorbates. This example illustrates the synchronization between the reactive-surface structure and its reactivity, and provides guidance for the synthesis process of alloy catalysts.

In addition, we acknowledge that the acceleration of the traditional path of catalyst exploration assisted by machine-learning techniques[76–80] has enabled more comprehensive material screening and more efficient catalyst design, illuminating the future of theory-guided catalysis.

Descriptors on metal-oxide surfaces

From the electronic and geometric standpoints, metal oxides are more complicated than metals and, hence, the development of descriptors for metal-oxide catalysts is more challenging than for metal catalysts. Electronically, the metal atoms can exhibit different oxidation states, which can lead to different catalytic properties. Geometrically, metal cations and oxygen anions can form various crystal structures, exposing a number of active sites with diverse local environments.

Metal-oxide catalysts are widely used for energy conversion[81–83]. For example, perovskite oxides (ABO_3 type) are applied in hydrogen production from water splitting[84–87] and in the ORR for fuel cells[88–90]. These applications arise from the unique electronic properties and controllable surface-binding energetics of perovskites. These electronic properties result from the hybridization of the d orbitals of the transition-metal atoms in the B sites with $2p$ atomic orbitals of oxygen, splitting into low-energy triplet t_{2g} orbitals that contain d_{xy}, d_{xz} and d_{yz} orbitals and high-energy doublet e_g orbitals containing d_{z^2} and $d_{x^2-y^2}$ orbitals[91]. To predict the oxygen evolution reaction (OER) intrinsic activity of perovskite oxides, it has been proposed that the occupation of antibonding states of the e_g orbitals is a more suitable descriptor than the number of $3d$ electrons of surface transition-metal atoms[92]. Using the e_g orbital descriptor is appropriate because the e_g orbital has a vertical orientation, which overlaps more favourably with the oxygen intermediates than the t_{2g} orbital does. There is a strong correlation between the occupancy of the e_g orbital and the binding energy of oxygen-related molecules on the B sites. Guided by this e_g-filling descriptor, a volcano-like

relationship was obtained between the OER catalytic activity and the occupancy of the e_g-symmetry orbital of the transition metal[93]. More specifically, a near-unity occupancy of the e_g orbital of the surface transition-metal ions enhances the intrinsic OER activity of perovskite transition-metal oxides. From the volcano plot, the perovskite oxide, $Ba_{0.5}Sr_{0.5}Co_{0.8}Fe_{0.2}O_{3-\delta}$, is located near the peak, which is consistent with the high activity of the OER by experiment (FIG. 3a). The application of a similar concept to electrocatalysis on transition-metal oxides with spinel structures[94] reconfirmed the role of electron orbital filling in metal-oxide catalysis.

For the ORR, the design principle for enhancing the ORR activity of transition-metal-oxide perovskites is to tune the e_g filling and the extent of B-site transition-metal–oxygen covalency[95]. In this study, a volcano plot was obtained using the e_g-filling descriptor and it was concluded that $e_g \approx 1$ is the most suitable condition for the ORR, with deviations from 1 hindering the kinetics of the reaction. In addition, the e_g-filling descriptor can be used to screen materials for other catalytic reactions and to predict the catalytic performance of reactions such as CO oxidation[91] and NO oxidation[96].

On the one hand, the e_g orbital filling of a transition metal such as Co is difficult to determine because of uncertain surface spintronic states[97]. On the other hand, according to descriptors based on molecular orbital theory, only transition-metal ions are considered as active sites, and electrons sharing metallic and oxygen sites in a covalent nature are also important for high-valence transition-metal ions. As a result, the development of perovskite-phase electronic structure descriptors is crucial. For perovskites, the antibonding orbital mainly derives from the $3d$ orbital of transition metal and the bonding orbital originates from oxygen $2p$ orbitals. As a consequence, it has been concluded that the covalency of the metal–oxygen bonds stabilizes the adsorbates and accelerates the kinetics of the reaction, thus enhancing ORR activity[95].

The p-band centre of bulk-phase oxygen has been used as a descriptor to describe the properties of the ORR on perovskite cathodes[98]. The O p-band centre is observed to have a good correlation with area-specific resistance, oxygen-exchange rates and other energetic information (more specifically, reaction energies and activation barriers related to ORR activity). Poor linear relationships in these systems were achieved when applying the common descriptors including the d-band centre. In addition, the O p-band centre is a bulk-phase property, which is more easily obtained than some surface information, owing to the complex nature of perovskite surfaces. In the OER, the O p-band centre also has a close correlation with the adsorption energy of the important intermediates. The high OER activity of double perovskites ($Ln_{0.5}Ba_{0.5}$)$CoO_{3-\delta}$ (Ln = Pr, Sm, Gd and Ho) in alkaline solution was attributed to the appropriate O p-band centre, which is neither too near nor too far from the Fermi level[99]. Moreover, perovskites with strong metal–oxygen covalency show higher OER activities with increasing pH[100].

As mentioned above, for catalytic reactions on metal oxides, and especially the oxidation of hydrocarbons, the

Electronic descriptors

a Surface descriptor

Structural descriptors

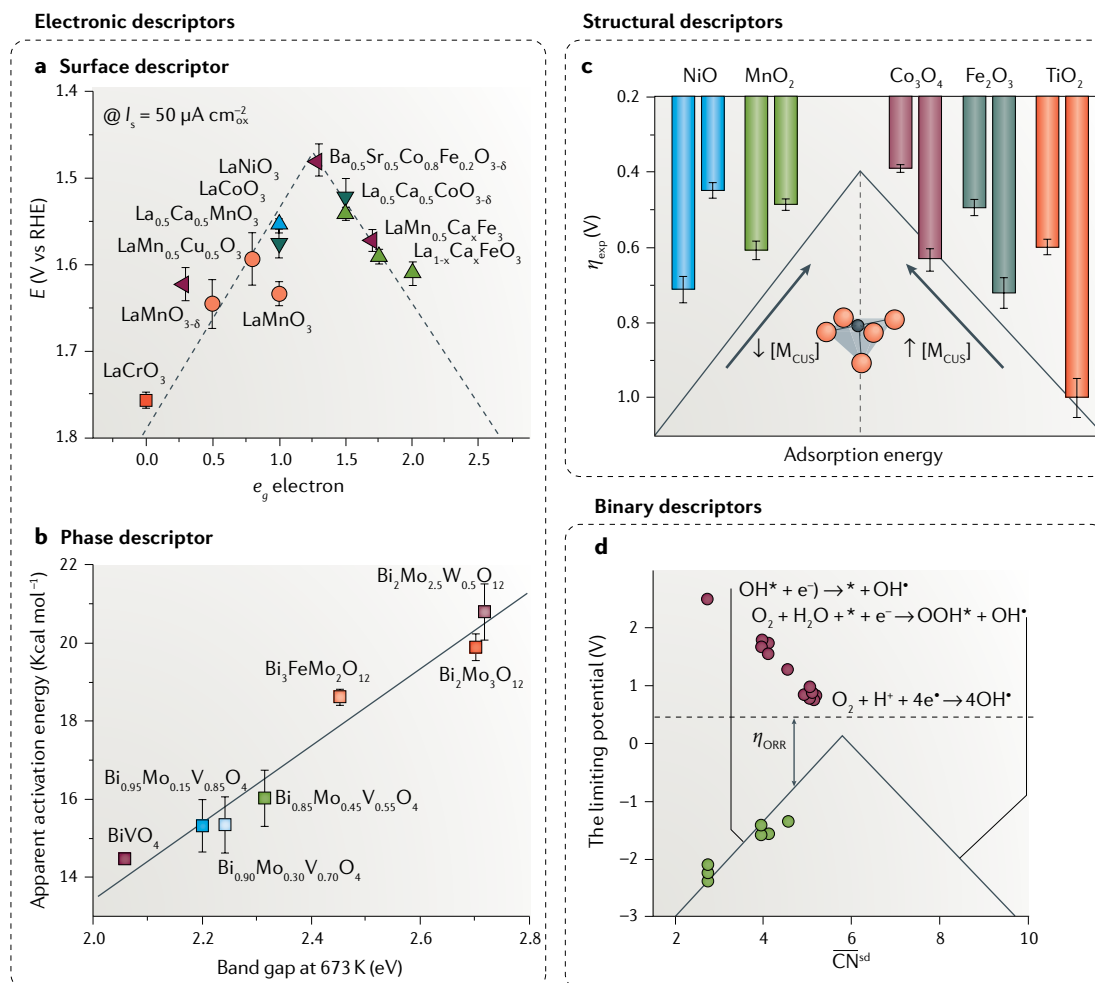**c**

b Phase descriptor

Binary descriptors

d

Fig. 3 | **Typical reactivity descriptors of metal-oxide catalysts. a** | An example of an electronic descriptor. A volcano plot depicting the relationship between the catalytic activity of the oxygen evolution reaction overpotential (E) as a function of the reversible hydrogen electrode (RHE) at $50\,\mu A\,cm_{ox}^{-2}$ (in which 'ox' represents the powder-oxide catalysts) of the surface-area-normalized kinetic current density (I_s) and the occupancy of the e_g-symmetry orbital of the transition metal (B in ABO$_3$). **b** | The linear relationship between apparent activation energies for the oxidation of propene to acrolein and the band gaps of the substituted bismuth molybdates at 673 K. **c** | A volcano plot of the overpotential in the oxygen evolution reaction as a function of the density of coordinatively unsaturated metal cation of transition-metal oxides (M$_{CUS}$). **d** | The relationship between binary descriptor $\overline{CN}^{sd}$ and the limiting potentials for two possible rate-determining steps on β-MnO$_2$ extended surfaces. The error bars in **a** and **c** indicate the measuring errors of the overpotential and in **b** denote the errors of apparent activation energy calculated from the measured reaction rate. Part **a** adapted with permission from REF.[93], AAAS. Part **b** is adapted with permission from REF.[101], American Chemical Society. Panel **c** is adapted from REF.[107], American Chemical Society. Panel **d** is adapted from REF.[108], American Chemical Society.

metal and oxygen components contribute to the reactivity. Therefore, both components must be taken into consideration to describe the catalytic activity. Band gap, as an important bulk property of the material, has been successfully applied as the descriptor to correlate with the activation energy of the rate-limiting step in propene oxidation on mixed-metal oxides[101] (FIG. 3b). Therefore, regulating both the average energy and the bandwidth of the metal d-orbital states can tune the band gap in mixed-metal oxides, which is correlated with the activation barriers of the key step of the oxidation reaction. To relate the oxygen-vacancy formation energies with intrinsic bulk properties, band gaps and the oxide enthalpy of formation were combined as descriptors of oxygen-vacancy formation in La$_x$Sr$_{1-x}$BO$_3$ perovskites

(where B = Cr, Mn, Fe, Co or Ni)[102]. A smaller band gap results in a lower energy of the oxygen-vacancy-induced defect band and the vacancy formation energy of oxygen decreases. Similarly, strained S-vacancies in the basal plane of 2H-phase monolayer MoS$_2$ were used to induce gap states. Superior HER activity can be obtained by optimizing a combination of strain and S-vacancies[103].

The adsorption energies (ΔE_{ADS}) of key intermediates including *O, *OH and *OOH on metal-oxide surfaces strongly influence the OER and ORR activity. Therefore, the correlation between the adsorption energies and the electronic structure of the metal oxides requires elucidation. Outer electrons of metal B in ABO$_3$-type perovskites, which is the number of remaining valence electrons of the oxidized-metal atom, were proposed

to describe this relationship[104]. Similar to the scaling relationships for different adsorbates on metal surfaces, it has been found that the binding energy of key intermediates such as *OH and *OOH on rutile-type oxide (TiO_2, IrO_2 and RuO_2) in the water-splitting reaction are linearly correlated with the binding energy of *O. If *O is strongly adsorbed on an oxide surface, *OH and *OOH also bond strongly on this surface. The slope of the linear relationship between the binding energy of *O and *OH on the metal-oxide and metal surfaces are similar (~0.6 and ~0.5, respectively). This scaling relationship can be extended to other metal oxides, for example, ABO_3-type perovskites. Similar to the metal surfaces, the scaling relationships on metal oxides can be explained by the d-band model. The addition of a hydrogen atom to atom Z weakens the ability of Z to couple with the d orbital of the metal and, therefore, fewer d states participate in coupling and the binding strength of ZH_x ($x > 0$) is weakened. The slope of the scaling relationship depends only on the identity of atom Z and the number of adsorbed hydrogen atoms[105].

CN and $\overline{CN}$ are structural descriptors of transition metals and describe the structure and electronic environment of an adsorption site[64,65,106]. However, the surfaces of transition-metal oxides are more complicated than the surfaces of metals. A descriptor termed the adjusted CN was suggested to predict the catalytic activity of metal oxides[72]. The adjusted CN involves the CN of the surface oxygen site (CN_O) and neighbouring metal atoms (ΣCN_M). The electronic and energetic properties of the active sites of five facets [(100), (110), (111), (211) and (311)] of four transition-metal oxides (V_2O_3, Cr_2O_3, Co_3O_4 and NiO) can be described based on this structural descriptor. Then, it is possible to predict the C–H activation energies (E_a) of alkane activation on Co_3O_4; more specifically, a linear relationship between the adjusted CN and E_a was found.

Transition-metal oxides, other than perovskites, are commonly used as catalysts for the OER. For these catalysts, descriptors based on e_g filling, which focus on the electronic properties of the catalysts, are typically considered and structural descriptors are investigated less. However, structural descriptors have been identified for transition-metal oxides; for example, one successful attempt is the application of the density of coordinatively unsaturated metal cations on oxide surfaces (M_{CUS})[107]. Surface structure can be tuned by varying the coverages of coordinatively unsaturated metal cations. It can be found that, by altering the M_{CUS} level, the adsorption of intermediate can be tuned, thus achieving the optimal OER activity (FIG. 3c). However, this structural descriptor fails to quantify the catalytic activity. To address this problem, a bond-energy-integrated orbital-wise CN ($\overline{CN}^{sd}$), which takes both geometrical and electronic effects into consideration, was proposed and employed as a binary descriptor for transition-metal oxides in oxygen-related electrochemical reactions[108] (FIG. 3d). In contrast to the CN^α (REF.[69]), $\overline{CN}^{sd}$ can quantitatively evaluate the bond energy of s and d orbitals. The scaling relationship between $\overline{CN}^{sd}$ and the adsorption energies of key intermediates can be established and, hence, the reactivity on transition-metal oxides can be accurately predicted.

Universal and other descriptors

Although most known reactivity descriptors in heterogeneous catalysis have focused on metal and metal-oxide catalysts, some studies have focused on other materials. For example, the catalytic principles and reactivity descriptors of carbon-based materials have been reviewed[109]. For these materials, the descriptors relevant for various electrochemical reactions are electron affinity and electronegativity[110,111], free energy of OH adsorption[112], free energy of iodine adsorption[111], position of the highest peak on the density of state of the active site[113], crystal-field stabilization energy[114] and π-electronic structure[115].

Until now, most of the reactivity descriptors described are limited to a single class of catalyst materials — that is, either metal surfaces, or metal-oxide surfaces or other surfaces. Hence, there is motivation to develop a universal reactivity descriptor. This motivation led researchers to consider simultaneously different reactions and to establish a descriptor appropriate for several reaction systems. For example, a trend was found in the adsorption of the ORR and OER intermediates, namely, *O, *OH and *OOH, when correlating these adsorption energies with the number of outer electrons[104] (FIG. 4a). Because the reactivity of the ORR and OER can be determined by the adsorption energies of *O and *OH, the number of outer electrons would be a good reactivity descriptor for ORRs and OERs not only on metals but also on metal oxides[116,117]. However, these attempts to find descriptors are limited to several material types and, hence, are regarded as semi-universal descriptors.

In one study, the construction of scaling relationships for over 20 types of catalysts, including different kinds of metals, metal oxides, cation-exchanged zeolites, decorated graphene nanosheets and metal-organic frameworks, was reported[118] (FIG. 4b). These scaling relationships correlated hydrogen affinity with transition-state energies of C–H bond activation. In addition, scaling relationships have been established between the formation energy of active sites and hydrogen affinity. The formation energy of active sites can be easily tuned by changing the physical properties of the catalysts. Thus, this universal descriptor can be used to determine whether a material can successfully activate methane and warrants testing experimentally.

To depict a comprehensive view of reactivity descriptors, we also summarize several descriptors for phosphide, carbide and sulfide catalysts. On doped MoP surfaces, there is a link between the stability of the P site and the adsorption energies of CH_x, NH_x and OH_x (REF.[119]). The dopants can tune the hybridization of the P site and then change the binding energies of adsorbates on the surfaces. In another example, the effect of surface non-metal doping on the HER activity of Ni_3P_2 termination of $Ni_2P(0001)$ was investigated using the random forest machine-learning algorithm[120]. The bond length of Ni–Ni was tuned, owing to a pressure-like effect on the Ni_3–hollow site induced by the non-metal dopants, and can be used to predict the activity of the HER reaction and to screen Ni–non-metal catalytic materials. For a mixture of metal and carbide surfaces, there is a volcano-shaped correlation between the catalytic activity

of the HER reaction and the surface energy. This correlation was identified by analysing the bulk and surface properties of six conventional catalysts (Au, Pd, Pt, WC, W_2C and Mo_2C) and nine hybrid catalysts (that is, the nine possible monolayer combinations of the
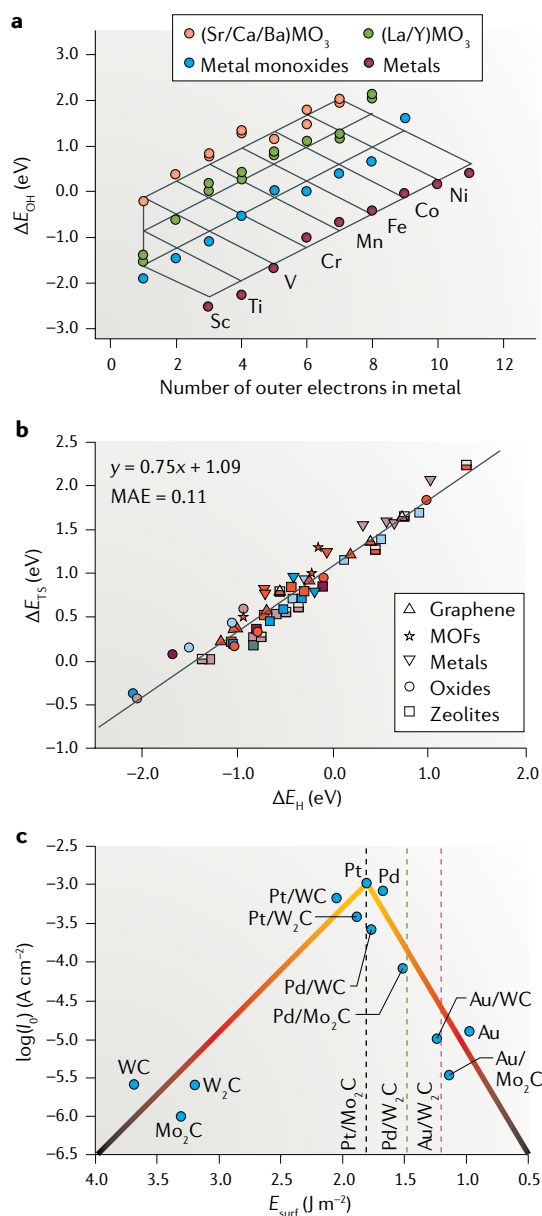

Fig. 4 | **Preliminary attempts to explore universal descriptors. a** | Adsorption energies of *OH (ΔE_{OH}) on metals, metal oxides and perovskites as a function of the number of outer electrons. **b** | The universal scaling relationship between hydrogenation affinity (ΔE_H) and the transition-state energy (ΔE_{TS}) of C–H bond breaking of methanol and five typical structures, namely, graphene, metal-organic frameworks (MOFs), metals, oxides and zeolites, with a mean absolute error (MAE) of 0.11. **c** | Experimental exchange-current densities (I_0) as a function of calculated surface energies (E_{surf}). Panel **a** is adapted with permission from REF.[104], Royal Society of Chemistry. Panel **b** is adapted from REF.[118], Springer Nature Limited. Panel **c** is adapted with permission from REF.[121], American Chemical Society.

three metals on the three transition-metal carbides substrates)[121] (FIG. 4c). Reactivity descriptors were also discovered in layered transition-metal sulfide catalysts. For these catalysts, the d-band centre of the edge-most metal site at the 0 monolayer of sulfur coverage is a general electronic descriptor for both structure and adsorption energies[122]. These energies can be used to predict the catalytic activity of sulfide catalysts.

For zeolite catalysts, the van der Waals interactions between the various alcohols and H-ZSM-5 have been selected to describe the activity of dehydration reactions[123]. Moreover, the van der Waals interactions correlate with the number of C atoms in the involved alcohols, which further facilitates the prediction of transition states of dehydration reactions. A descriptor-based approach for the adsorption of CO and NO on the Cu, Ni, Co and Fe sites of zeolites (SSZ-13 and MOR) was also developed[124]. Using a machine-learning genetic algorithm, the positions of metal s orbitals, the number of valence electrons and the energy gap between the highest occupied molecular orbital and the lowest unoccupied molecular orbital of the adsorbates were identified as the most important parameters to establish appropriate descriptors. The heat of adsorption of ammonia $\Delta H_{ADS}(NH_3)$ can also be used as a reactivity descriptor on zeotype catalysts[125,126].

The development of descriptors for single-atom catalysts is a popular area of research. The well-defined active centre of single-atom catalysts provides a good basis on which theoreticians can model the structure and predict the activity, which brings researchers closer to accurate structure–reactivity relationships and reactivity descriptors[71,127–141]. For graphene-based single-atom catalysts, a universal design principle was presented to evaluate the activity of electrocatalysts towards the ORRs, OERs and HERs[71]. The activity of such catalysts correlates with the local environment of the metal centre, including the CN and the electronegativity of the nearest-neighbour atoms, which has been validated by experimental results. Another example is the effects of dopants in ceria catalysts for C–C coupling of CO_2 and CH_4 (REF.[142]). There is a positive linear relationship between the activation barrier and the electronegativity of the doped metals (Al, Zn, Cd, In, Ga or Ni). As a result, the electronegativity of the dopants can be used as a reactivity descriptor to predict the C–C coupling activation barriers on doped ceria catalysts.

How to break scaling relationships

Descriptors based on scaling relationships are powerful tools to predict the catalytic properties of active sites and to screen for new catalysts. Reaction intermediates bind to the surface with predictable strength, which can be obtained easily from established scaling relationships of adsorption energies. Specifically, the BEP relationship indicates a linear correlation between the activation barrier and the reaction energy of a reaction step, making reactions predictable. However, the established relationships also constrain the catalytic performance of active sites, making it difficult to achieve low activation barriers and weak intermediate adsorption at the same time, thus limiting the development of optimal catalysts.

Researchers have been attempting to break the scaling relationship for the past decade. By decorating transition-metal surfaces with a second catalytic site, LiH, the scaling relationships that limit the performance of ammonia synthesis on conventional transition metals can be broken[143]. LiH is also a surface modifier, which changes the chemical properties of the original surfaces. A similar method was used to modify Pt catalysts with sulfide addition to disproportionally tune the binding strength of the key intermediates *OOH and *OH[144]. Modifying active sites with additives can promote reactivity by modifying reaction pathways. Scaling relations can also be broken by introducing tensile strain to the reactive surfaces[145]. A mechanics-based eigenstress model was applied to scrutinize the effect of artificial strain on the binding strength of different reaction intermediates. This method assumes that the relative energy between the initial state (IS) and the transition state (TS) is altered via uniaxial loading (FIG. 5a). The dimerization of N atoms to form N_2 on Pt(100) was studied as an example reaction (FIG. 5b). By applying uniaxial compression, the expansive Poisson response is favourable for the TS, while the IS is destabilized. The introduction of surface tensile strain reduces the energy barrier by decreasing the TS energy and increasing the IS energy, and, hence, the confinement of the BEP relation is broken.

Another way to break the scaling relationships is to use single-atom catalysts[146]. Inspired by homogeneous catalysts and biological enzymes, researchers have fabricated heterogeneous catalysts featuring highly dispersed reactive-metal centres such as Pt, Rh, Ru, Ni and other single-atom catalysts[147–150]. For example, the single-atom catalysts commonly have reactive centres surrounded by inert atoms; thus, the reactants can dissociate on the reactive-metal atoms and the products can easily desorb from the coordination sites.

The chemical properties endowed by the atomic arrangement breaks the scaling relationships of single-atom catalysts for many different reactions. Both in situ electron spectroscopy and DFT calculations demonstrate the sharpness of free-atom-like d states of the isolated element in single-atom catalysts, as a consequence of weak hybridization with the surrounding coordination environment. Therefore, these single-atom sites bind adsorbates in a similar manner as molecular metal complexes[151]. This finding unveils the possibility to design free-atom-like active sites that previously only appeared in homogeneous catalysis and, hence, to boost the reactivity of single-atom catalysts. The free-atom-like electronic structure of Pt/Cu single-atom alloy (SAA) was also discussed[70,152], and the projected density of states of Pt atoms on different surfaces can be seen in FIG. 5c. The prominently sharp peak of Pt atoms in SAA Pt/Cu(111) confirms the special electronic structure of the isolated metal atoms in single-atom catalysts. Based on the unique electronic property, the performance of single-atom catalyst Pt/Cu was tested in multiple reactions. For example, with the aid of Pt/Cu SAA catalysts, the scaling relationship for propane dehydrogenation reactions can be broken[132] (FIG. 5d). In this work, DFT calculations show that the Pt/Cu SAA catalyst favours desorption of propylene rather than further hydrogenation and maintains a moderate activation barrier for the dehydrogenation of propane. Hence, the performance of the Pt/Cu SAA catalyst breaks the established scaling relationship for PtM (where M = 3d and 4d transition metals) alloys. The propane dehydrogenation experiments catalysed by such alloys demonstrate that the Pt/Cu SAA catalyst enhances both the propylene selectivity and propane conversion compared with PtM alloy surfaces. The isolated Pt atoms are suitable active sites for the dehydrogenation of propane, and the surrounding Cu sites facilitate the desorption of propylene. This example illustrates the ability of single-atom catalysts to break the confinement of scaling relationships. Furthermore, the support of the single-metal atoms can modify the oxidation states of the isolated atoms, which further alters the established scaling relationships, as illustrated by the atomically dispersed Rh on phosphotungstic acid during CO oxidation[153].

The breaking of scaling relationships is actually the discovery of catalysts following another scaling relationship. In other words, breaking scaling relationships is an attempt to locate another scaling line and find the optimal zones on the new plot, for example, a higher volcano peak of activity or selectivity than on the previous plot. Including the methods to break the scaling discussed above, the molecular-mediated, electrochemical, proton-coupled electron-transfer reactions can be improved by changing the properties of reactants and products, instead of modifying the catalyst[154]. The slopes of scaling relationships vary as the parameters of ORR catalysis differ. Thus, by changing the intrinsic properties of input and output molecules, old scaling relationships can be broken and new scaling correlations can be built. By coupling catalysts to a non-thermal plasma, the scaling relationship in ammonia synthesis can also be circumvented, owing to the activation of certain degrees of freedom of gas molecules[130]. To conclude, there are valuable approaches to address the limitation of scaling relationships: by introducing ligands, surface strain, non-thermal plasma and other external forces to the catalytic systems or by designing single-atom catalysts with unique electronic structures. These factors help to identify excellent catalytic performance beyond the scaling relationship.

Outlook

The ability of scaling relationships to simplify our understanding of catalysis inspires us to extract specific reactivity descriptors to predict the reaction trends and to screen for new catalysts. However, the complexity of catalytic systems leads to numerous reactivity descriptors, which are specifically explored to describe certain sections of the catalysis. The strategies to break the scaling relationships are still not sufficient and it is difficult to find a way to improve the catalytic performance of complex reaction systems. Technically, the available computational capacity is not satisfactory to meet the demands of DFT calculations to explore complex reaction networks, which limit the progress in catalyst screening and rational design. Moreover, as our insight into catalysis deepens, a universal reactivity descriptor for multi-catalytic systems is gaining attention.

Development of universal descriptors

Most descriptors are not transferable and, hence, researchers are tasked with discovering numerous parameters for different reactions, which hampers the effectiveness of theory-guided catalysis. The *d*-band centre is one of the most successful descriptors, but it does not apply to metal oxides and other catalysts. Generalized CNs are powerful for metal particles, but fail to function for interface catalysis, which requires both the metal and the support to be considered. The formation energy of active sites is a potential candidate, because the formation energy of a specific active site can be tuned by changing the physical properties of the catalyst[118]. At present, the goal is to develop reactivity descriptors that can be used simultaneously in various types of catalyst and reaction systems, namely, universal descriptors. A successful
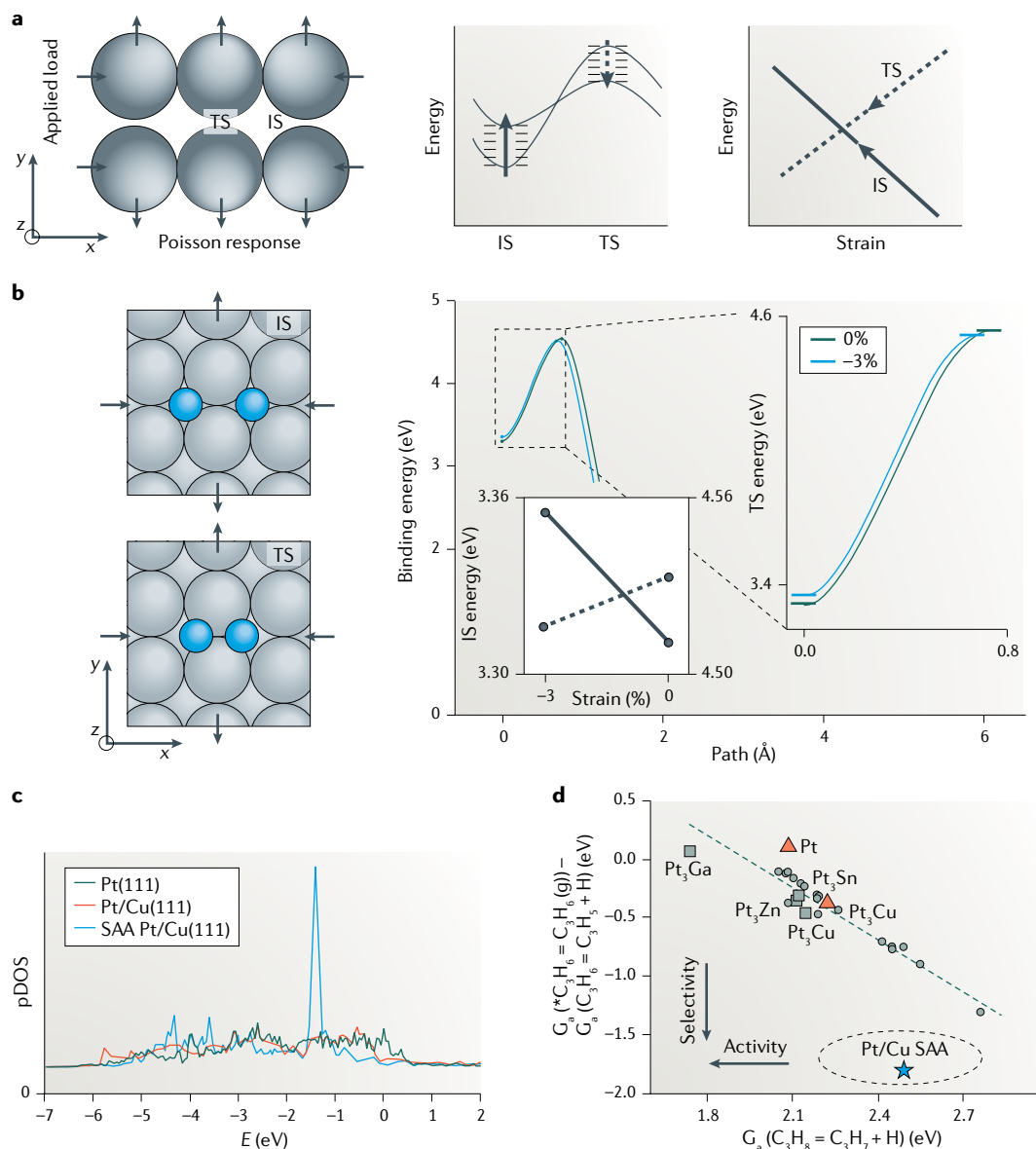
Fig. 5 | **Methods to break the scaling relationships in heterogeneous catalysis. a** | A schematic depicting the surface strain of applying a uniaxial compression to the surface (left). A qualitative plot of the energy-level changes of the initial state (IS) and the transition state (TS) with the applied loading of uniaxial compression (middle). A plot of the binding energy of the IS and the TS as a function of strain reveals the expected violation of TS scaling (right). **b** | Schematic diagrams of the N_2 association reaction (left) and results of climbing-image nudged elastic band (CI-NEB) calculations displaying the response of the IS and the TS to a uniaxial compressive load (right). **c** | Projected density of state (pDOS) for the *d* band of surface Pt atoms in Pt(111) (green), Pt/Cu(111) (red) and single-atom alloy (SAA) Pt/Cu(111) (blue). **d** | Screening of Pt-based bimetallic catalysts for propane dehydrogenation (PDH) by using the scaling relationship between the first dehydrogenation free-energy barrier (representing PDH activity) and the propylene desorption free-energy barrier divided by the deep dehydrogenation free-energy barrier (representing PDH selectivity), where G_a is the Gibbs energy barrier. The formation of isolated Pt atoms on a SAA Pt/Cu surface successfully breaks the traditional scaling with enhanced activity and selectivity. Panels **a** and **b** are adapted from REF.[145], Springer Nature Limited. Panel **c** is adapted with permission from REF.[70], American Chemical Society. Panel **d** is adapted from REF.[131], Springer Nature Limited.

example of the universal descriptor is the numbers and electronegativities of atoms in the local environment of the metal centre, denoted as φ[71], which has been applied to the design of single-atom electrocatalysts. In the short term, the discovery of a universal reactivity descriptor for all materials and reactions is not achievable, but it is possible to extract regionally universal descriptors, which are accurate for catalytic reactions within a subfield, such as the ORR, the OER or dehydrogenation. These descriptors may expand to other reactions, which is crucial for the fulfilment of a globally universal descriptor.

Breaking the scaling relationships

We have discussed the importance of breaking scaling relationships to enable the discovery of optimal catalysts. When a scaling relationship is broken, a different scaling relationship is established. The method typically used to break scaling relationships is to modify the reactive sites artificially or form single-atom catalysts to disproportionally alter the adsorption trends of key intermediates. In addition, modulating reaction conditions or the properties of reactants and products can help to remove the restriction on activity and selectivity.

Screening strategy. Descriptor-based screening methods have been identified to replace the trial-and-error experimental exploration process. However, reactivity descriptors originate from time-consuming DFT calculations. With the help of the degree of rate control analysis[155,156], the complex reaction network is simplified by identifying the key elementary steps of the network. Nascent machine-learning techniques may break through the bottleneck of basic DFT calculation processes[31]. Big data from DFT calculations is particularly suitable for the machine-learning process. By providing these training data, machine-learning techniques can offer accurate potential energies that can match the quality of electronic structure calculations. With the development of computing hardware and optimization of machine-learning programs, we are ready for machine-learning-based methods to accelerate DFT calculations[157–162]. Maintaining both accuracy and efficiency, we are looking forward to more trials using machine-learning methods to automate and accelerate the discovery of reactivity descriptors.

Published online 21 November 2019

1. Ertl, G. Reactions at surfaces: from atoms to complexity (Nobel Lecture). *Angew. Chem. Int. Ed.* **47**, 3524–3535 (2008).
2. Nørskov, J. K. et al. Universality in heterogeneous catalysis. *J. Catal.* **209**, 275–278 (2002).
3. Mizuno, N. & Misono, M. Heterogeneous catalysis. *Chem. Rev.* **98**, 199–218 (1998).
4. Hammer, B. & Nørskov, J. K. Why gold is the noblest of all the metals. *Nature* **376**, 238–240 (1995).
5. Nørskov, J. K. Electronic is factors in catalysis. *Prog. Surf. Sci.* **38**, 103–144 (1991).
6. Nilsson, A. et al. The electronic structure effect in heterogeneous catalysis. *Catal. Lett.* **100**, 111–114 (2005).
7. Nørskov, J. K., Bligaard, T., Rossmeisl, J. & Christensen, C. H. Towards the computational design of solid catalysts. *Nat. Chem.* **1**, 37–46 (2009).
8. Curtarolo, S. et al. The high-throughput highway to computational materials design. *Nat. Mater.* **12**, 191–201 (2013).
9. Montemore, M. M. & Medlin, J. W. Scaling relations between adsorption energies for computational screening and design of catalysts. *Catal. Sci. Technol.* **4**, 3748–3761 (2014).
10. Greeley, J. Theoretical heterogeneous catalysis: scaling relationships and computational catalyst design. *Annu. Rev. Chem. Biomol. Eng.* **7**, 605–635 (2016).
11. Hammer, B., Morikawa, Y. & Norskov, J. K. CO chemisorption at metal surfaces and overlayers. *Phys. Rev. Lett.* **76**, 2141–2144 (1996).
12. Nørskov, J. K., Abild-Pedersen, F., Studt, F. & Bligaard, T. Density functional theory in surface chemistry and catalysis. *Proc. Natl Acad. Sci. USA* **108**, 937–943 (2011).
13. Hammer, B. & Nørskov, J. K. Theoretical surface science and catalysis—calculations and concepts. *Adv. Catal.* **45**, 71–129 (2000).
14. Kitchin, J. R., Nørskov, J. K., Barteau, M. A. & Chen, J. G. Modification of the surface electronic and chemical properties of Pt(111) by subsurface 3*d* transition metals. *J. Chem. Phys.* **120**, 10240–10246 (2004).
15. Greeley, J. & Mavrikakis, M. Alloy catalysts designed from first principles. *Nat. Mater.* **3**, 810–815 (2004).
16. Kitchin, J. R., Nørskov, J. K., Barteau, M. A. & Chen, J.G. Role of strain and ligand effects in the modification of the electronic and chemical properties of bimetallic surfaces. *Phys. Rev. Lett.* **93**, 156801 (2004).
17. Cai, W. et al. Subsurface catalysis-mediated selectivity of dehydrogenation reaction. *Sci. Adv.* **4**, eaar5418 (2018).
18. Xin, H., Vojvodic, A., Voss, J., Nørskov, J. K. & Abild-Pedersen, F. Effects of *d*-band shape on the surface reactivity of transition-metal alloys. *Phys. Rev. B* **89**, 15114 (2014).
19. Visikovskiy, A. et al. Electronic *d*-band properties of gold nanoclusters grown on amorphous carbon. *Phys. Rev. B* **83**, 165428 (2011).
20. Logadottir, A. et al. The Brønsted–Evans–Polanyi relation and the volcano plot for ammonia synthesis over transition metal catalysts. *J. Catal.* **197**, 229–231 (2001).
21. Wang, S. et al. Universal Brønsted–Evans–Polanyi relations for C–C, C–O, C–N, N–O, N–N, and O–O dissociation reactions. *Catal. Lett.* **141**, 370–373 (2010).
22. Nørskov, J. K. et al. The nature of the active site in heterogeneous metal catalysis. *Chem. Soc. Rev.* **37**, 2163–2171 (2008).
23. Michaelides, A. et al. Identification of general linear relationships between activation energies and enthalpy changes for dissociation reactions at surfaces. *J. Am. Chem. Soc.* **125**, 3704–3705 (2003).
24. Bligaard, T. et al. The Brønsted–Evans–Polanyi relation and the volcano curve in heterogeneous catalysis. *J. Catal.* **224**, 206–217 (2004).
25. Loffreda, D., Delbecq, F., Vigne, F. & Sautet, P. Fast prediction of selectivity in heterogeneous catalysis from extended Brønsted–Evans–Polanyi relations: a theoretical insight. *Angew. Chem. Int. Ed.* **48**, 8978–8980 (2009).
26. Vojvodic, A. et al. On the behavior of Brønsted–Evans–Polanyi relations for transition metal oxides. *J. Chem. Phys.* **134**, 244509 (2011).
27. Wang, S. et al. Universal transition state scaling relations for (de)hydrogenation over transition metals. *Phys. Chem. Chem. Phys.* **13**, 20760–20765 (2011).
28. Viñes, F., Vojvodic, A., Abild-Pedersen, F. & Illas, F. Brønsted–Evans–Polanyi relationship for transition metal carbide and transition metal oxide surfaces. *J. Phys. Chem. C* **117**, 4168–4171 (2013).
29. Yang, B., Burch, R., Hardacre, C., Headdock, G. & Hu, P. Understanding the optimal adsorption energies for catalyst screening in heterogeneous catalysis. *ACS Catal.* **4**, 182–186 (2013).
30. Fajín, J. L. C., Cordeiro, M. N. D. S., Illas, F. & Gomes, J. R. B. Generalized Brønsted–Evans–Polanyi relationships and descriptors for O–H bond cleavage of organic molecules on transition metal surfaces. *J. Catal.* **313**, 24–33 (2014).
31. Kitchin, J. R. Machine learning in catalysis. *Nat. Catal.* **1**, 230–232 (2018).
32. Marti, S. et al. Computational design of biological catalysts. *Chem. Soc. Rev.* **37**, 2634–2643 (2008).
33. Behler, J. Constructing high-dimensional neural network potentials: a tutorial review. *Int. J. Quantum Chem.* **115**, 1032–1050 (2015).
34. Brockherde, F. et al. Bypassing the Kohn–Sham equations with machine learning. *Nat. Commun.* **8**, 872 (2017).
35. Ramprasad, R., Batra, R., Pilania, G., Mannodi-Kanakkithodi, A. & Kim, C. Machine learning in materials informatics: recent applications and prospects. *npj Comput. Mater.* **3**, 54 (2017).
36. Klanner, C. et al. The development of descriptors for solids: teaching "catalytic intuition" to a computer. *Angew. Chem. Int. Ed.* **116**, 5461–5463 (2004).
37. Back, S. et al. Convolutional neural network of atomic surface structures to predict binding energies for high-throughput screening of catalysts. *J. Phys. Chem. Lett.* **10**, 4401–4408 (2019).
38. Abild-Pedersen, F. et al. Scaling properties of adsorption energies for hydrogen-containing molecules on transition-metal surfaces. *Phys. Rev. Lett.* **99**, 016105 (2007).
39. Calle-Vallejo, F., Martínez, J. I., García-Lastra, J. M., Rossmeisl, J. & Koper, M. T. Physical and chemical nature of the scaling relations between adsorption energies of atoms on metal surfaces. *Phys. Rev. Lett.* **108**, 116103 (2012).
40. Stamenkovic, V. et al. Changing the activity of electrocatalysts for oxygen reduction by tuning the surface electronic structure. *Angew. Chem. Int. Ed.* **118**, 2963–2967 (2006).
41. Mavrikakis, M., Hammer, B. & Nørskov, J. K. Effect of strain on the reactivity of metal surfaces. *Phys. Rev. Lett.* **81**, 2819–2822 (1998).
42. Zhou, Y. et al. Dopant-induced electron localization drives CO_2 reduction to C_2 hydrocarbons. *Nat. Chem.* **10**, 974–980 (2018).
43. Sabatier, P. Hydrogénations et déshydrogénations par catalyse. *Ber. Dtsch. Chem. Ges.* **44**, 1984–2001 (1911).
44. Medford, A. J. et al. From the Sabatier principle to a predictive theory of transition-metal heterogeneous catalysis. *J. Catal.* **328**, 36–42 (2015).
45. Laursen, A. B. et al. Electrochemical hydrogen evolution: Sabatier's principle and the volcano plot. *J. Chem. Educ.* **89**, 1595–1599 (2012).
46. Huang, B. et al. A CO adsorption site change induced by copper substitution in a ruthenium catalyst for enhanced CO oxidation activity. *Angew. Chem. Int. Ed.* **131**, 2252–2257 (2019).
47. Kattel, S., Ramirez, P. J., Chen, J. G., Rodriguez, J. A. & Liu, P. Active sites for CO_2 hydrogenation to methanol on Cu/ZnO catalysts. *Science* **355**, 1296–1299 (2017).
48. Greeley, J. et al. Alloys of platinum and early transition metals as oxygen reduction electrocatalysts. *Nat. Chem.* **1**, 552–556 (2009).
49. Lima, F. H. B. et al. Catalytic activity–*d*-band center correlation for the O_2 reduction reaction on platinum in alkaline solutions. *J. Phys. Chem. C* **111**, 404–410 (2007).
50. Greeley, J., Jaramillo, T. F., Bonde, J., Chorkendorff, I. & Nørskov, J. K. Computational high-throughput screening of electrocatalytic materials for hydrogen evolution. *Nat. Mater.* **5**, 909–913 (2006).

51. Zhang, Y.-J., Sethuraman, V., Michalsky, R. & Peterson, A. A. Competition between CO_2 reduction and H_2 evolution on transition-metal electrocatalysts. *ACS Catal.* **4**, 3742–3748 (2014).

52. Cave, E. R. et al. Trends in the catalytic activity of hydrogen evolution during CO_2 electroreduction on transition metals. *ACS Catal.* **8**, 3035–3040 (2018).

53. Greeley, J., Nørskov, J. K., Kibler, L. A., El-Aziz, A. M. & Kolb, D. M. Hydrogen evolution over bimetallic systems: understanding the trends. *ChemPhysChem* **7**, 1032–1035 (2006).

54. Tran, K. & Ulissi, Z. W. Active learning across intermetallics to guide discovery of electrocatalysts for CO_2 reduction and H_2 evolution. *Nat. Catal.* **1**, 696–703 (2018).

55. Studt, F. et al. Identification of non-precious metal alloy catalysts for selective hydrogenation of acetylene. *Science* **320**, 1320–1322 (2008).

56. Wang, W., Wang, S., Ma, X. & Gong, J. Recent advances in catalytic hydrogenation of carbon dioxide. *Chem. Soc. Rev.* **40**, 3703–3727 (2011).

57. Studt, F. et al. Discovery of a Ni-Ga catalyst for carbon dioxide reduction to methanol. *Nat. Chem.* **6**, 320–324 (2014).

58. Jia, C. et al. Catalytic chemistry predicted by a charge polarization descriptor: synergistic O_2 activation and CO oxidation by Au–Cu bimetallic clusters on $TiO_2(101)$. *ACS Appl. Mater. Interfaces* **11**, 9629–9640 (2019).

59. Dickens, C. F., Montoya, J. H., Kulkarni, A. R., Bajdich, M. & Nørskov, J. K. An electronic structure descriptor for oxygen reactivity at metal and metal-oxide surfaces. *Surf. Sci.* **681**, 122–129 (2019).

60. Kirlin, P. S. & Gates, B. C. Activation of the C–C bond provides a molecular basis for structure sensitivity in metal catalysis. *Nature* **325**, 38–40 (1987).

61. Carberry, J. Structure sensitivity in heterogeneous catalysis: activity and yield/selectivity. *J. Catal.* **114**, 277–283 (1988).

62. Haruta, M. When gold is not noble: catalysis by nanoparticles. *Chem. Rec.* **3**, 75–87 (2003).

63. Gustafson, J. et al. Sensitivity of catalysis to surface structure: the example of CO oxidation on Rh under realistic conditions. *Phys. Rev. B* **78**, 045423 (2008).

64. Calle-Vallejo, F., Loffreda, D., Koper, M. T. & Sautet, P. Introducing structural sensitivity into adsorption–energy scaling relations by means of coordination numbers. *Nat. Chem.* **7**, 403–410 (2015).

65. Calle-Vallejo, F. et al. Finding optimal surface sites on heterogeneous catalysts by counting nearest neighbors. *Science* **350**, 185–189 (2015).

66. Zhu, W. et al. Low-coordinated edge sites on ultrathin palladium nanosheets boost carbon dioxide electroreduction performance. *Angew. Chem. Int. Ed.* **57**, 11544–11548 (2018).

67. Choksi, T. S., Roling, L. T., Streibel, V. & Abild-Pedersen, F. Predicting adsorption properties of catalytic descriptors on bimetallic nanoalloys with site-specific precision. *J. Phys. Chem. Lett.* **10**, 1852–1859 (2019).

68. Jinnouchi, R. & Asahi, R. Predicting catalytic activity of nanoparticles by a DFT-aided machine-learning algorithm. *J. Phys. Chem. Lett.* **8**, 4279–4283 (2017).

69. Ma, X. & Xin, H. Orbitalwise coordination number for predicting adsorption properties of metal nanocatalysts. *Phys. Rev. Lett.* **118**, 036101 (2017).

70. Zhao, Z. J., Mu, R., Wang, X. & Gong, J. Fast prediction of CO binding energy via the local structure effect on PtCu alloy surfaces. *Langmuir* **33**, 8700–8706 (2017).

71. Xu, H., Cheng, D., Cao, D. & Zeng, X. C. A universal principle for a rational design of single-atom electrocatalysts. *Nat. Catal.* **1**, 339–348 (2018).

72. Fung, V., Tao, F. F. & Jiang, D. E. General structure–reactivity relationship for oxygen on transition-metal oxides. *J. Phys. Chem. Lett.* **8**, 2206–2211 (2017).

73. Strmcnik, D., Lopes, P. P., Genorio, B., Stamenkovic, V. R. & Markovic, N. M. Design principles for hydrogen evolution reaction catalyst materials. *Nano Energy* **29**, 29–36 (2016).

74. Chattot, R. et al. Surface distortion as a unifying concept and descriptor in oxygen reduction reaction electrocatalysis. *Nat. Mater.* **17**, 827–833 (2018).

75. Liu, S. et al. Adsorption preference determines segregation direction: a shortcut to more realistic surface models of alloy catalysts. *ACS Catal.* **9**, 5011–5018 (2019).

76. Ulissi, Z. W. et al. Machine-learning methods enable exhaustive searches for active bimetallic facets and reveal active site motifs for CO_2 reduction. *ACS Catal.* **7**, 6600–6608 (2017).

77. Medford, A. J., Kunz, M. R., Ewing, S. M., Borders, T. & Fushimi, R. Extracting knowledge from data through catalysis informatics. *ACS Catal.* **8**, 7403–7429 (2018).

78. Jinnouchi, R., Hirata, H. & Asahi, R. Extrapolating energetics on clusters and single-crystal surfaces to nanoparticles by machine-learning scheme. *J. Phys. Chem. C* **121**, 26397–26405 (2017).

79. Li, Z., Wang, S., Chin, W. S., Achenie, L. E. & Xin, H. High-throughput screening of bimetallic catalysts enabled by machine learning. *J. Mater. Chem. A* **5**, 24131–24138 (2017).

80. Schlexer Lamoureux, P. et al. Machine learning for computational heterogeneous catalysis. *ChemCatChem* **11**, 3581–3601 (2019).

81. Wang, H. et al. Bifunctional non-noble metal oxide nanoparticle electrocatalysts through lithium-induced conversion for overall water splitting. *Nat. Commun.* **6**, 7261 (2015).

82. Li, Y. H. et al. Local atomic structure modulations activate metal oxide as electrocatalyst for hydrogen evolution in acidic water. *Nat. Commun.* **6**, 8064 (2015).

83. Liu, X. et al. Noble metal–metal oxide nanohybrids with tailored nanostructures for efficient solar energy conversion, photocatalysis and environmental remediation. *Energy Environ. Sci.* **10**, 402–434 (2017).

84. Han, B. et al. Iron-based perovskites for catalyzing oxygen evolution reaction. *J. Phys. Chem. C* **122**, 8445–8454 (2018).

85. Vojvodic, A. & Nørskov, J. K. Optimizing perovskites for the water-splitting reaction. *Science* **334**, 1355–1356 (2011).

86. Wang, J. et al. Water splitting with an enhanced bifunctional double perovskite. *ACS Catal.* **8**, 364–371 (2017).

87. Han, X., Yu, Y., Huang, Y., Liu, D. & Zhang, B. Photogenerated carriers boost water splitting activity over transition-metal/semiconducting metal oxide bifunctional electrocatalysts. *ACS Catal.* **7**, 6464–6470 (2017).

88. Kim, N. I. et al. Oxygen-deficient triple perovskites as highly active and durable bifunctional electrocatalysts for oxygen electrode reactions. *Sci. Adv.* **4**, eaap9360 (2018).

89. Jung, S., McCrory, C. C. L., Ferrer, I. M., Peters, J. C. & Jaramillo, T. F. Benchmarking nanoparticulate metal oxide electrocatalysts for the alkaline water oxidation reaction. *J. Mater. Chem. A* **4**, 3068–3076 (2016).

90. Liu, X. et al. High-performance non-spinel cobalt–manganese mixed oxide-based bifunctional electrocatalysts for rechargeable zinc–air batteries. *Nano Energy* **20**, 315–325 (2016).

91. Hwang, J. et al. Perovskites in catalysis and electrocatalysis. *Science* **358**, 751–756 (2017).

92. Hong, W. T. et al. Toward the rational design of non-precious transition metal oxides for oxygen electrocatalysis. *Energy Environ. Sci.* **8**, 1404–1427 (2015).

93. Suntivich, J., May, K. J., Gasteiger, H. A., Goodenough, J. B. & Shao-Horn, Y. A perovskite oxide optimized for oxygen evolution catalysis from molecular orbital principles. *Science* **334**, 1383–1385 (2011).

94. Wei, C. et al. Cations in octahedral sites: a descriptor for oxygen electrocatalysis on transition-metal spinels. *Adv. Mater.* **29**, 1606800 (2017).

95. Suntivich, J. et al. Design principles for oxygen-reduction activity on perovskite oxide catalysts for fuel cells and metal–air batteries. *Nat. Chem.* **3**, 546–550 (2011).

96. Choi, S. O., Penninger, M., Kim, C. H., Schneider, W. F. & Thompson, L. T. Experimental and computational investigation of effect of Sr on NO oxidation and oxygen exchange for $La_{1-x}Sr_xCoO_3$ perovskite catalysts. *ACS Catal.* **3**, 2719–2728 (2013).

97. Haverkort, M. W. et al. Spin state transition in $LaCoO_3$ studied using soft X-ray absorption spectroscopy and magnetic circular dichroism. *Phys. Rev. Lett.* **97**, 176405 (2006).

98. Lee, Y.-L., Kleis, J., Rossmeisl, J., Shao-Horn, Y. & Morgan, D. Prediction of solid oxide fuel cell cathode activity with first-principles descriptors. *Energy Environ. Sci.* **4**, 3966–3970 (2011).

99. Grimaud, A. et al. Double perovskites as a family of highly active catalysts for oxygen evolution in alkaline solution. *Nat. Commun.* **4**, 2439 (2013).

100. Grimaud, A. et al. Activating lattice oxygen redox reactions in metal oxides to catalyse oxygen evolution. *Nat. Chem.* **9**, 457–465 (2017).

101. Getsoian, A. B., Zhai, Z. & Bell, A. T. Band-gap energy as a descriptor of catalytic activity for propene oxidation over mixed metal oxide catalysts. *J. Am. Chem. Soc.* **136**, 13684–13697 (2014).

102. Deml, A. M., Stevanović, V., Muhich, C. L., Musgrave, C. B. & O'Hayre, R. Oxide enthalpy of formation and band gap energy as accurate descriptors of oxygen vacancy formation energetics. *Energy Environ. Sci.* **7**, 1996–2004 (2014).

103. Li, H. et al. Activating and optimizing MoS_2 basal planes for hydrogen evolution through the formation of strained sulphur vacancies. *Nat. Mater.* **15**, 48–53 (2016).

104. Calle-Vallejo, F. et al. Number of outer electrons as descriptor for adsorption processes on transition metals and their oxides. *Chem. Sci.* **4**, 1245–1249 (2013).

105. Fernandez, E. M. et al. Scaling relationships for adsorption energies on transition metal oxide, sulfide, and nitride surfaces. *Angew. Chem. Int. Ed.* **47**, 4683–4686 (2008).

106. Calle-Vallejo, F., Martínez, J. I., García-Lastra, J. M., Sautet, P. & Loffreda, D. Fast prediction of adsorption properties for platinum nanocatalysts with generalized coordination numbers. *Angew. Chem. Int. Ed.* **53**, 8316–8319 (2014).

107. Tao, H. B. et al. Identification of surface reactivity descriptor for transition metal oxides in oxygen evolution reaction. *J. Am. Chem. Soc.* **138**, 9978–9985 (2016).

108. Wu, D., Dong, C., Zhan, H. & Du, X. W. Bond-energy-integrated descriptor for oxygen electrocatalysis of transition metal oxides. *J. Phys. Chem. Lett.* **9**, 3387–3391 (2018).

109. Zhang, L. et al. Guiding principles for designing highly efficient metal-free carbon catalysts. *Adv. Mater.* **31**, 1805252 (2019).

110. Zhao, Z., Li, M., Zhang, L., Dai, L. & Xia, Z. Design principles for heteroatom-doped carbon nanomaterials as highly efficient catalysts for fuel cells and metal–air batteries. *Adv. Mater.* **27**, 6834–6840 (2015).

111. Zhao, Z., Lin, C.-Y., Tang, J. & Xia, Z. Catalytic mechanism and design principles for heteroatom-doped graphene catalysts in dye-sensitized solar cells. *Nano Energy* **49**, 193–199 (2018).

112. Zhang, J., Zhao, Z., Xia, Z. & Dai, L. A metal-free bifunctional electrocatalyst for oxygen reduction and oxygen evolution reactions. *Nat. Nanotechnol.* **10**, 444–452 (2015).

113. Zheng, Y. et al. Hydrogen evolution by a metal-free electrocatalyst. *Nat. Commun.* **5**, 3783 (2014).

114. Lin, C. Y., Zhang, L., Zhao, Z. & Xia, Z. Design principles for covalent organic frameworks as efficient electrocatalysts in clean energy conversion and green oxidizer production. *Adv. Mater.* **29**, 1606635 (2017).

115. Sinthika, S., Waghmare, U. V. & Thapa, R. Structural and electronic descriptors of catalytic activity of graphene-based materials: first-principles theoretical analysis. *Small* **14**, 1703609 (2018).

116. Nørskov, J. K. et al. Origin of the overpotential for oxygen reduction at a fuel-cell cathode. *J. Phys. Chem. B* **108**, 17886–17892 (2004).

117. Man, I. C. et al. Universality in oxygen evolution electrocatalysis on oxide surfaces. *ChemCatChem* **3**, 1159–1165 (2011).

118. Latimer, A. A. et al. Understanding trends in C–H bond activation in heterogeneous catalysis. *Nat. Mater.* **16**, 225–229 (2017).

119. Fields, M. et al. Scaling relations for adsorption energies on doped molybdenum phosphide surfaces. *ACS Catal.* **7**, 2528–2534 (2017).

120. Wexler, R. B., Martirez, J. M. P. & Rappe, A. M. Chemical pressure-driven enhancement of the hydrogen evolving activity of Ni_2P from nonmetal surface doping interpreted via machine learning. *J. Am. Chem. Soc.* **140**, 4678–4683 (2018).

121. Zhuang, H., Tkalych, A. J. & Carter, E. A. Surface energy as a descriptor of catalytic activity. *J. Phys. Chem. C* **120**, 23698–23706 (2016).

122. Tsai, C., Chan, K., Nørskov, J. K. & Abild-Pedersen, F. Understanding the reactivity of layered transition-metal sulfides: a single electronic descriptor for structure and adsorption. *J. Phys. Chem. Lett.* **5**, 3884–3889 (2014).

123. Fečík, M., Plessow, P. N. & Studt, F. Simple scheme to predict transition-state energies of dehydration reactions in zeolites with relevance to biomass conversion. *J. Phys. Chem. C* **122**, 23062–23067 (2018).

124. Göltl, F., Müller, P., Uchupalanun, P., Sautet, P. & Hermans, I. Developing a descriptor-based approach for CO and NO adsorption strength to transition metal sites in zeolites. *Chem. Mater.* **29**, 6434–6444 (2017).

REVIEWS

125. Wang, C. M., Brogaard, R. Y., Weckhuysen, B. M., Nørskov, J. K. & Studt, F. Reactivity descriptor in solid acid catalysis: predicting turnover frequencies for propene methylation in zeotypes. *J. Phys. Chem. Lett.* **5**, 1516–1521 (2014).
126. Brogaard, R. Y., Wang, C.-M. & Studt, F. Methanol–alkene reactions in zeotype acid catalysts: insights from a descriptor-based approach and microkinetic modeling. *ACS Catal.* **4**, 4504–4509 (2014).
127. Wang, A., Li, J. & Zhang, T. Heterogeneous single-atom catalysis. *Nat. Rev. Chem.* **2**, 65–81 (2018).
128. Marcinkowski, M. D. et al. Pt/Cu single-atom alloys as coke-resistant catalysts for efficient C−H activation. *Nat. Chem.* **10**, 325–332 (2018).
129. Zhang, Z. et al. Thermally stable single atom Pt/m-Al_2O_3 for selective hydrogenation and CO oxidation. *Nat. Commun.* **8**, 16100 (2017).
130. Mehta, P. et al. Overcoming ammonia synthesis scaling relations with plasma-enabled catalysis. *Nat. Catal.* **1**, 269–275 (2018).
131. Sun, G. et al. Breaking the scaling relationship via thermally stable Pt/Cu single atom alloys for catalytic dehydrogenation. *Nat. Commun.* **9**, 4454 (2018).
132. Nie, L. et al. Activation of surface lattice oxygen in single-atom Pt/CeO_2 for low-temperature CO oxidation. *Science* **358**, 1419–1423 (2017).
133. Liu, J. et al. Tackling CO poisoning with single-atom alloy catalysts. *J. Am. Chem. Soc.* **138**, 6396–6399 (2016).
134. Lucci, F. R. et al. Selective hydrogenation of 1,3-butadiene on platinum–copper alloys at the single-atom limit. *Nat. Commun.* **6**, 8550 (2015).
135. Qiao, B. et al. Single-atom catalysis of CO oxidation using Pt1/FeO_x. *Nat. Chem.* **3**, 634–641 (2011).
136. Bruix, A. et al. Maximum noble-metal efficiency in catalytic materials: atomically dispersed surface platinum. *Angew. Chem. Int. Ed.* **53**, 10525–10530 (2014).
137. Wei, H. et al. FeO_x-supported platinum single-atom and pseudo-single-atom catalysts for chemoselective hydrogenation of functionalized nitroarenes. *Nat. Commun.* **5**, 5634 (2014).
138. Zhang, S. et al. Catalysis on singly dispersed bimetallic sites. *Nat. Commun.* **6**, 7938 (2015).
139. Cheng, M.-J., Clark, E. L., Pham, H. H., Bell, A. T. & Head-Gordon, M. Quantum mechanical screening of single-atom bimetallic alloys for the selective reduction of CO_2 to C_1 hydrocarbons. *ACS Catal.* **6**, 7769–7777 (2016).
140. Lin, L. et al. A highly CO-tolerant atomically dispersed Pt catalyst for chemoselective hydrogenation. *Nat. Nanotechnol.* **14**, 354–361 (2019).
141. Liu, D. et al. Atomically dispersed platinum supported on curved carbon supports for efficient electrocatalytic hydrogen evolution. *Nat. Energy* **4**, 512–518 (2019).
142. Zhao, Y. et al. Simultaneous activation of CH_4 and CO_2 for concerted C−C coupling at oxide–oxide interfaces. *ACS Catal.* **9**, 3187–3197 (2019).
143. Wang, P. et al. Breaking scaling relations to achieve low-temperature ammonia synthesis through LiH-mediated nitrogen transfer and hydrogenation. *Nat. Chem.* **9**, 64–70 (2017).
144. Wang, Y. Y., Chen, D. J., Allison, T. C. & Tong, Y. J. Effect of surface-bound sulfide on oxygen reduction reaction on Pt: breaking the scaling relationship and mechanistic insights. *J. Chem. Phys.* **150**, 041728 (2019).
145. Khorshidi, A., Violet, J., Hashemi, J. & Peterson, A. A. How strain can break the scaling relations of catalysis. *Nat. Catal.* **1**, 263–268 (2018).
146. Darby, M. T., Stamatakis, M., Michaelides, A. & Sykes, E. C. H. Lonely atoms with special gifts: breaking linear scaling relationships in heterogeneous catalysis with single-atom alloys. *J. Phys. Chem. Lett.* **9**, 5636–5646 (2018).
147. Ye, S. et al. Highly stable single Pt atomic sites anchored on aniline-stacked graphene for hydrogen evolution reaction. *Energy Environ. Sci.* **12**, 1000–1007 (2019).
148. Therrien, A. J. et al. An atomic-scale view of single-site Pt catalysis for low-temperature CO oxidation. *Nat. Catal.* **1**, 192–198 (2018).
149. Jeong, H. et al. Fully dispersed Rh ensemble catalyst to enhance low-temperature activity. *J. Am. Chem. Soc.* **140**, 9558–9565 (2018).
150. Jiang, K. et al. Isolated Ni single atoms in graphene nanosheets for high-performance CO_2 reduction. *Energy Environ. Sci.* **11**, 893–903 (2018).
151. Greiner, M. T. et al. Free-atom-like *d* states in single-atom alloy catalysts. *Nat. Chem.* **10**, 1008–1015 (2018).
152. Thirumalai, H. & Kitchin, J. R. Investigating the reactivity of single atom alloys using density functional theory. *Top. Catal.* **61**, 462–474 (2018).
153. Hülsey, M. J. et al. In situ spectroscopy-guided engineering of rhodium single-atom catalysts for CO oxidation. *Nat. Commun.* **10**, 1330 (2019).
154. Pegis, M. L., Wise, C. F., Koronkiewicz, B. & Mayer, J. M. Identifying and breaking scaling relations in molecular catalysis of electrochemical reactions. *J. Am. Chem. Soc.* **139**, 11000–11003 (2017).
155. Stegelmann, C., Andreasen, A. & Campbell, C. T. Degree of rate control: how much the energies of intermediates and transition states control rates. *J. Am. Chem. Soc.* **131**, 8077–8082 (2009).
156. Wolcott, C. A., Medford, A. J., Studt, F. & Campbell, C. T. Degree of rate control approach to computational catalyst screening. *J. Catal.* **330**, 197–207 (2015).
157. Yao, K., Herr, J. E., Toth, D. W., McKintyre, R. & Parkhill, J. The TensorMol-0.1 model chemistry: a neural network augmented with long-range physics. *Chem. Sci.* **9**, 2261–2269 (2018).
158. Kolb, B., Lentz, L. C. & Kolpak, A. M. Discovering charge density functionals and structure-property relationships with PROPhet: a general framework for coupling machine learning and first-principles methods. *Sci. Rep.* **7**, 1192 (2017).
159. Khorshidi, A. & Peterson, A. A. Amp: a modular approach to machine learning in atomistic simulations. *Comput. Phys. Commun.* **207**, 310–324 (2016).
160. Artrith, N. & Urban, A. An implementation of artificial neural-network potentials for atomistic materials simulations: performance for TiO_2. *Comput. Mater. Sci.* **114**, 135–150 (2016).
161. Behler, J. Atom-centered symmetry functions for constructing high-dimensional neural network potentials. *J. Chem. Phys.* **134**, 074106 (2011).
162. Behler, J. & Parrinello, M. Generalized neural-network representation of high-dimensional potential-energy surfaces. *Phys. Rev. Lett.* **98**, 146401 (2007).

Author contributions
J.G., Z.-J.Z., S.Z., S.L. and D.C. wrote the manuscript. All the authors participated in the revising of the manuscript.

Competing interests
The authors declare no competing interests.

Publisher's note
Springer Nature remains neutral with regard to jurisdictional claims in published maps and institutional affiliations.